



Synthesis, microstructure and characterization of ultra-low permittivity CuO–ZnO–B₂O₃–Li₂O glass/Al₂O₃ composites for ULTCC application

Juan Xi^a, Guohua Chen^{a,*}, Fei Liu^b, Fei Shang^a, Jiwen Xu^a, Changrong Zhou^a, Changlai Yuan^a

^a School of Material Science and Engineering, Guangxi Key Laboratory of Information Materials, Guilin University of Electronic Technology, Guilin, 541004, China

^b School of Mechanical and Electrical Engineering, Guilin University of Electronic Technology, Guilin, 541004, PR China

ARTICLE INFO

Keywords:

Composites

LTCC

Dielectric properties

ABSTRACT

In view of lead-free low-softening CuO–ZnO–B₂O₃–Li₂O glass, novel glass/Al₂O₃ ceramic composites were prepared by solid-state reaction route for ultra-low temperature co-fired ceramic (ULTCC) applications. The phase evolution and compositions, microstructure and microwave dielectric properties of the composites were studied by XRD, SEM and dielectric property measurement. Four phases including Cu₂Al₆B₄O₁₇, Li₂CuB₄O₈, CuB₂O₄ and Al₂O₃ coexist in the glass/Al₂O₃ ceramic composites sintered in the range of 640–660 °C. However, the contents and types of the phases depend on the composition of the composites and firing temperature. The optimum properties with a permittivity $\epsilon_r = 3.79$, a quality factor $Q \times f = 38557 \text{ GHz}$ (at 16.64 GHz) and a temperature coefficient of resonance frequency $\tau_f \approx 0 \text{ ppm/}^\circ\text{C}$ as well as a heat conductivity $\lambda = 1.46 \text{ W (mK)}^{-1}$ can be achieved for the glass/ceramic composite containing 10 wt% Al₂O₃ sintered at 640 °C. Moreover, the composite can be co-fired compatible with Ag and Al electrodes. The as-prepared glass/Al₂O₃ ceramic composites are promising candidate for ULTCC application.

1. Introduction

Along with the progress of modern wireless communication technology, microwave communication components and modules have gradually become the most important part, and the high wiring density, high volumetric efficiency, high signal-transmission speed, and low cost are needed [1–5]. Ultralow or low-temperature co-fired ceramic (ULTCC, LTCC) technology provides an effective and low-cost way for electronic components and devices to be tightly arranged in multilayer ceramic structures [6–10].

The sintering temperature of co-fired ceramics must be lower than the melting point of Ag, Al metal electrodes, and the metal electrodes and LTCC substrate ceramics can be chemically compatible [11–17].

As is known to all, Al₂O₃ is the most commonly used substrate material in the electronics industry because of its good mechanical, chemical and abrasion resistance, high hardness, low loss [18]. However, Al₂O₃ substrate has a larger permittivity (~ 10) high sintering temperature, which increases signal transmission time and co-firing with Ag and Al electrodes cannot be realized. S. J. Perm et al. [19] studied the dielectric constant and dielectric loss of alumina sintered in air at 1000 °C and 1600 °C for 5 and 1800 min. Therefore, it is urgent to develop new substrate materials with low sintering temperature, low dielectric constant, low loss and near zero τ_f .

To realize the required dielectric properties and densification at low sintering temperature, the most commonly used method is to prepare the glass/ceramic composite [20]. The low softening temperature glasses such as ZnO–B₂O₃ glass, PbO–B₂O₃–SiO₂ glass, CuO–B₂O₃–Li₂O glass [21–23], etc, serve as a densification additive to improve densification, and the ceramic filler such as Al₂O₃ plays a role in regulating the physical properties of the resulting composites. In fact, to reduce the sintering temperature, the crystallizable glass with low melting point and low glass transition temperature usually is added to ceramic which has a high sintering temperature, and the crystallizable glass plays a role of reducing the sintering temperature and achieving densification in the glass/ceramic composite. As we all know, compared with amorphous glass, crystalline phase with the same chemical composition has smaller dielectric loss. Therefore, crystallizable glass not only improves ceramic densification, but also precipitates crystalline phase with low dielectric loss, which can effectively decrease the dielectric loss of composite material [10,24]. X.Y. Chen et al. [24] reported a new composite based on the crystallizable La₂O₃–B₂O₃–Al₂O₃ glass/Al₂O₃ for LTCC applications. La₂O₃–B₂O₃–Al₂O₃ glass has low softening point and controllable crystallization properties. Recently, our research group found a new crystallizable CuO–ZnO–B₂O₃–Li₂O (CZBL) glass with low softening temperature and controllable crystallization character, and the CZBL glass fired at 620 °C possesses optimum properties with

* Corresponding author.

E-mail address: cgh1682002@163.com (G. Chen).

<https://doi.org/10.1016/j.ceramint.2019.08.166>

Received 28 July 2019; Received in revised form 12 August 2019; Accepted 17 August 2019

0272-8842/ © 2019 Elsevier Ltd and Techna Group S.r.l. All rights reserved.

Table 1
Compositions of the CZBL glass/ Al_2O_3 compositions (wt%).

Sample	Al_2O_3	CZBL glass
A1	5	95
A2	10	90
A3	15	85

$\epsilon_r = 3.33$, $Q \times f = 17724 \text{ GHz}$ and $\tau_f \approx 0 \text{ ppm/}^\circ\text{C}$ [25]. In this study, a series of CZBL glass/ Al_2O_3 composites with 5–15 wt% Al_2O_3 were synthesized, and their phase compositions, microstructure, and physical properties were discussed. In addition, the co-firing compatibility between the composite and Ag, Al electrode was also investigated for LTCC application.

2. Experimental procedure

The glass composition is $16\text{CuO}-16\text{ZnO}-63\text{B}_2\text{O}_3-5\text{Li}_2\text{O}$ (CZBL, wt %). The initial reagent-grade raw materials of CuO and ZnO ($\geq 99\%$, Xilong Chemical Reagent Co., Ltd, China), H_3BO_3 ($\geq 99.5\%$, Guanghai Sci-Tech Co. Ltd, China) and Li_2CO_3 ($\geq 99.5\%$, Aladdin Chemical Reagent Company) were dried and weighed according to the above glass composition. The mixed batch was kept in a high temperature furnace at 1150°C for 1 h to get glass liquid, and then the glass melt is poured into water quenched to obtain glass slag. The glass slag was ball ground for 6 h in a ball mill at a speed of 300r/min. The resulting glass powders were dried at 100°C for 8 h. The composition ratio of CZBL glass/ Al_2O_3 ($\geq 99\%$, Xilong Chemical Reagent Co., Ltd, China) composites is listed in Table 1. Al_2O_3 and CZBL glass powders mixed for 24 h with zirconia balls using alcohol as a medium. The uniform mixture was pressed uniaxially under 5 MPa pressure to make a pellet with 12 mm in diameter and 6 mm in height. Then, the pellets were sintered at $580-680^\circ\text{C}$ for 1 h with a heating rate of 4°C/min .

The phase of the sintered composite was measured by powder X-ray diffraction (Bruker, D8-Advance, Germany) with Cu K α radiation ($\lambda = 1.5406 \text{ \AA}$) in the 2θ range $15-80^\circ$. The bulk density was measured by Archimedeian method. The microstructures of the sintered specimens, which were polished and etched in HF (5 vol%) for 30 s, were examined by field emission scanning electron microscope (Quanta, FEG450, America) equipped with energy dispersion spectroscopy (EDS). The microwave dielectric properties were measured by a Vector Network Analyzer (Agilent Technologies, N5230C, America). The value of temperature coefficient of resonance frequency (τ_f) was gained among $25^\circ\text{C}-75^\circ\text{C}$ using the following formula:

$$\tau_f = \frac{(f_{75} - f_{25}) \times 10^6}{50 \times f_{25}} \text{ ppm/}^\circ\text{C} \quad (1)$$

where f_{75} and f_{25} are the resonant frequencies at 75°C and 25°C , respectively. The thermal diffusivity (α) was obtained via a conductometer (Netzsch, LFA467, Germany). The specific heat (C_p) was examined by the differential scanning calorimeter (Ta, DSC-250, America). The thermal conductivity can be obtained from this formula: $\lambda = \alpha \rho C_p$.

3. Results and discussion

Fig. 1(a) exhibits XRD patterns of sample A1 sintered at different temperatures. At 580°C , only crystalline phase is Al_2O_3 in the composite, as shown in Fig. 1(a). With further increasing temperature to 600°C , the secondary phase $\text{Cu}_2\text{Al}_6\text{B}_4\text{O}_{17}$ emerges besides Al_2O_3 , indicating that the CZBL glass reacts with ceramic filler Al_2O_3 . The reaction mechanism may be proposed as follows: $\text{CuO} + \text{B}_2\text{O}_3 + \text{Al}_2\text{O}_3$

$\text{Cu}_2\text{Al}_6\text{B}_4\text{O}_{17}$. Plachinda et al. [26] synthesized $\text{Cu}_2\text{Al}_6\text{B}_4\text{O}_{17}$ compounds and found the morphology of $\text{Cu}_2\text{Al}_6\text{B}_4\text{O}_{17}$ shows whiskers. When sintered at 620°C , the third phase $\text{Li}_2\text{CuB}_4\text{O}_8$ precipitates from

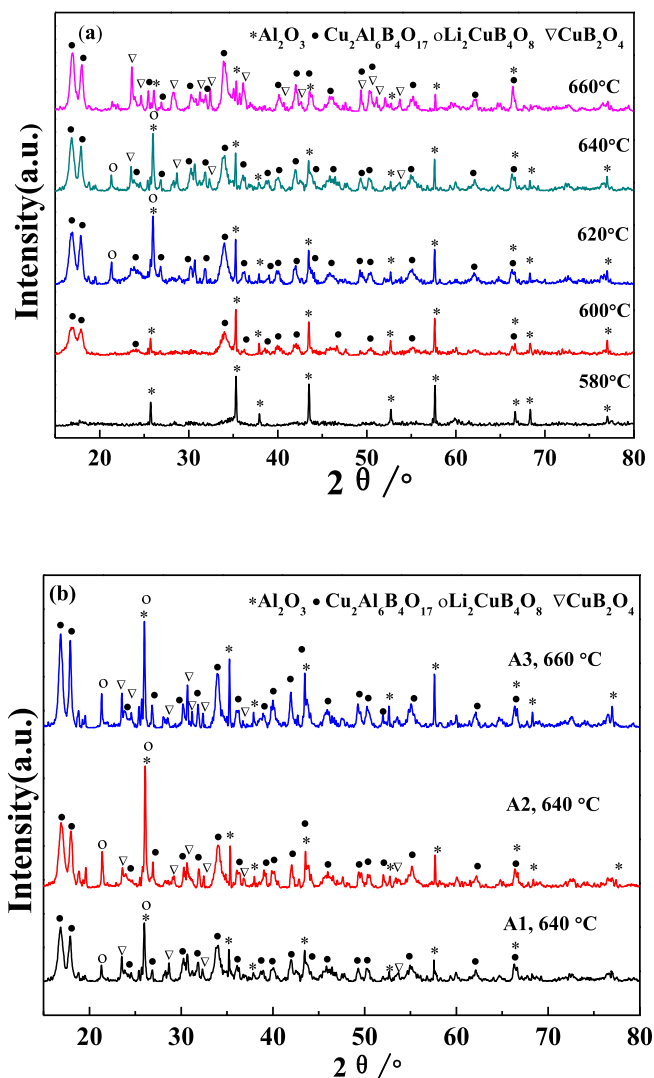


Fig. 1. XRD patterns of sample A1 sintered at different temperatures (a) and samples A1, A2, A3 sintered at optimum firing temperature (b).

the glass matrix in the composite. With further increasing temperature in the range of $640^\circ\text{C}-660^\circ\text{C}$, the CuB_2O_4 phase appears and the diffraction intensity of CuB_2O_4 obviously increases with the increment of sintering temperature. Here, four phases including Al_2O_3 , $\text{Cu}_2\text{Al}_6\text{B}_4\text{O}_{17}$, $\text{Li}_2\text{CuB}_4\text{O}_8$ and CuB_2O_4 coexist. Fig. 1(b) shows the XRD analysis results of A1, A2 and A3 sintered at optimum temperatures. All composite samples are comprised of $\text{Cu}_2\text{Al}_6\text{B}_4\text{O}_{17}$, $\text{Li}_2\text{CuB}_4\text{O}_8$, CuB_2O_4 and Al_2O_3 phases. However, the relative amounts of the phases vary with different content of ceramic and firing temperatures.

Fig. 2 indicates SEM images of fracture surface of A1-A3 sintered at different conditions. From Fig. 2(a), A1 sample sintered at 580°C shows more glass phase, in other words, the content of crystal phases is low. With increasing temperature to 600°C , the microstructure becomes dense and the contents of crystal phases increase, as shown in Fig. 2(b). With further increasing temperature to 620°C , the contents of crystal phases sequentially increase, especially, some whisker phases emerge, as seen in Fig. 2(c). When the sintering temperature is increased to 640°C , a large number of homogeneous whiskers is observed and the dense microstructure can be obtained, as shown in Fig. 2(d). At 660°C , the grain sizes in the composite obviously grow shown in Fig. 2(e). Zhu et al. [27] reported the reaction process of $\text{Cu}_2\text{Al}_6\text{B}_4\text{O}_{17}$ whiskers and found that $\text{Cu}_2\text{Al}_6\text{B}_4\text{O}_{17}$ whiskers develop through three stages: nanoparticles, fan-shaped whiskers and agminate-needlelike whiskers. Based

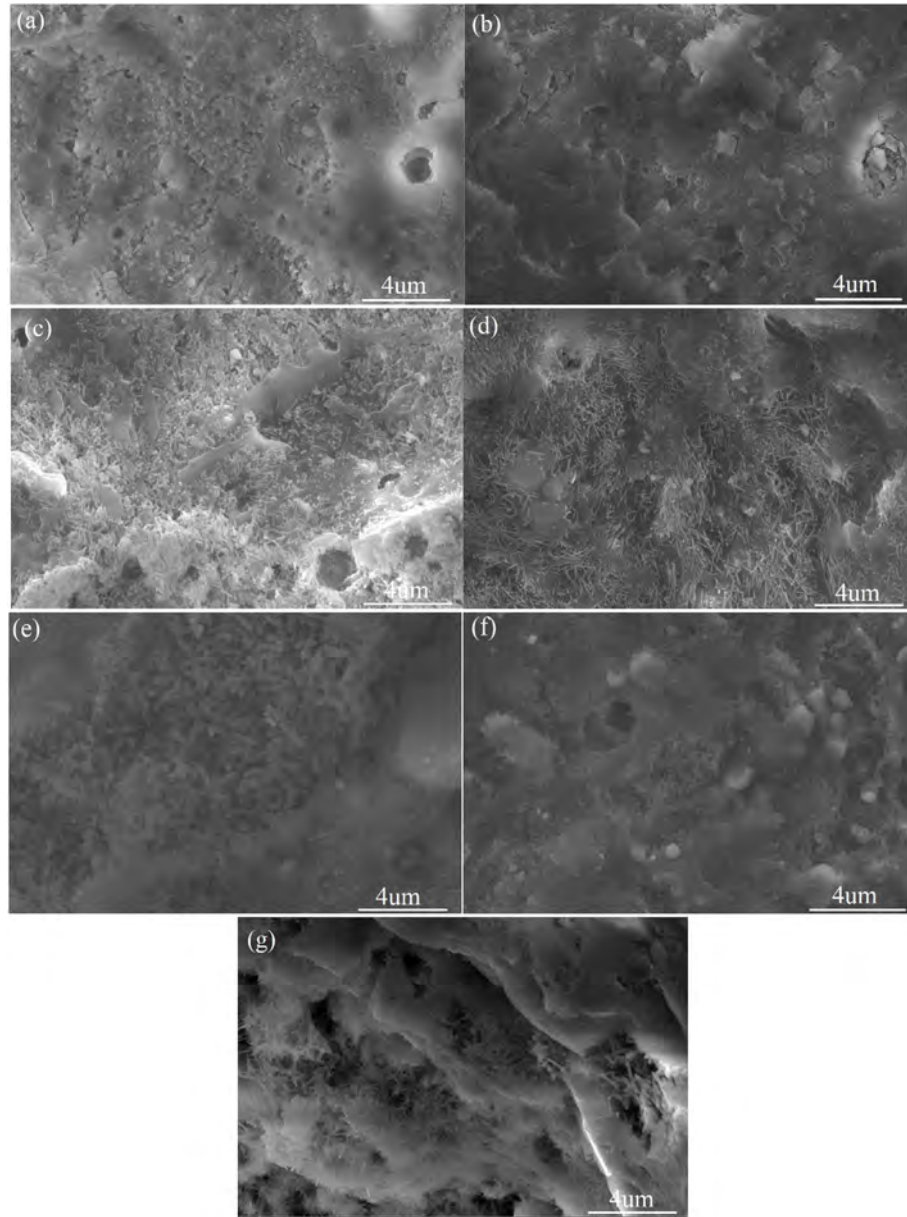


Fig. 2. SEM micrographs of fracture surface of A2 sintered at different temperatures for 1h: (a)580 °C; (b) 600 °C; (c) 620 °C; (d)640 °C; (e)660 °C; (f)A1 sintered at 640 °C; (g)A3 sintered at 660 °C.

on the XRD results, it can be inferred the whiskers observed in Fig. 2 is $\text{Cu}_2\text{Al}_6\text{B}_4\text{O}_{17}$ phases. In general, for the same sample, the increase of temperature favors the densification of the composite during sintering process. However, excessive firing temperature plays the opposite role in the densification. It is also found the composite with different Al_2O_3 has respective optimum sintering temperature, and similarly, $\text{Cu}_2\text{Al}_6\text{B}_4\text{O}_{17}$ whiskers are observed, as shown in Figs. (f) and (g).

The bulk densities of CZBL glass/ Al_2O_3 composites sintered at different temperature are shown in Fig. 3. It is clear that the density firstly increases and then decreases with the increment of sintering temperature. However, the optimal sintering temperature varies with different composite sample. As mentioned earlier, CZBL glass has a low softening and crystallization temperature. During sintering, the solid particles can be wetted and tightened by the liquid phase, at the same time, solid particles slip and rearrange and the sample gets to be dense. Moreover, some crystal phase precipitate from glass phase, and the chemical reaction occurs between CZBL glass and Al_2O_3 , which conversely increases viscosity and then prevents the sintering densification.

Therefore, too much or too little addition of glass is improper. The bulk densities of A2 are distinctly higher than that of the other two composites.

The mixture of ideal dielectrics can be simply considered as a multilayer material, each layer parallel or perpendicular to the applied electric field. When each layer is parallel to the capacitor plate, the structure is equivalent to the series connection of many capacitor elements, and the reciprocal of the total capacitance is equal to the sum of the reciprocal capacitance of each layer. The following formula is obtained:

$$\frac{1}{k'} = \frac{v_1}{k'_1} + \frac{v_2}{k'_2} \frac{1}{k'} = \frac{v_1}{k'_1} + \frac{v_2}{k'_2} \quad (2)$$

Where v_1 and v_2 represent the volume fraction of crystalline phases. However, When the arrangement of the components is perpendicular to the capacitor plate, the applied electric field can be added directly to each component:

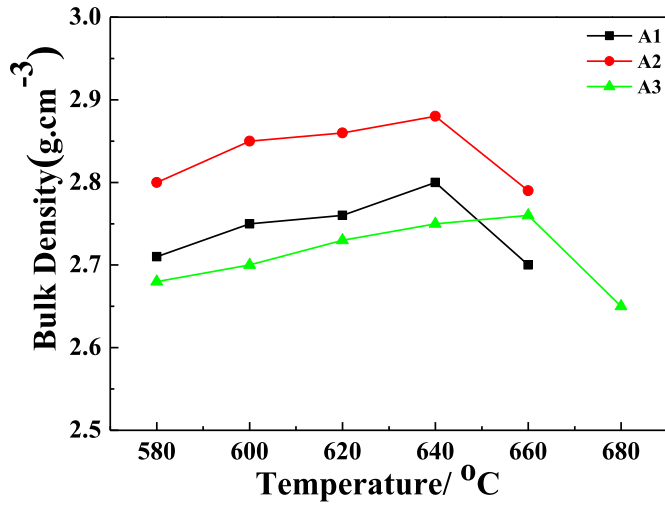


Fig. 3. Bulk densities of A1, A2 and A3 as a function of sintering temperature.

$$k' = v_1 k_1' + v_2 k k' = v_1 k + v_2 k \quad (3)$$

Formula (2) and (3) are special cases of the following general empirical relations:

$$k^n = \sum_i k_i k_i^n \quad (4)$$

For equation (2), $n = -1$, for equation (3), $n = +1$, v_i is the volume integral of phase i .

$$\log k = \sum_i v_i \log k_i \quad (5)$$

This is the logarithm rule, the values are between the extremum given by formula (2) and (3).

The A1, A2 and A3 composites are made up of ceramic phase, glass phase and pores, therefore the following equation was obtained:

$$\log k_{\text{composites}} = v_{\text{ceramic}} \log k_{\text{ceramic}} + v_{\text{glass}} \log k_{\text{glass}} + v_{\text{pores}} \log k_{\text{pores}} \quad (6)$$

Generally, the permittivity depends on the density, ionic polarizability, microstructure, porosity and secondary. The permittivity of CZBL glass/ Al_2O_3 composites sintered at different temperatures is exhibited in Fig. 4. It is clearly that the ϵ_r value has a similar trend to the bulk density of the composites shown in Fig. 3. It can be found that the permittivity of all the composites increases with sintering temperature

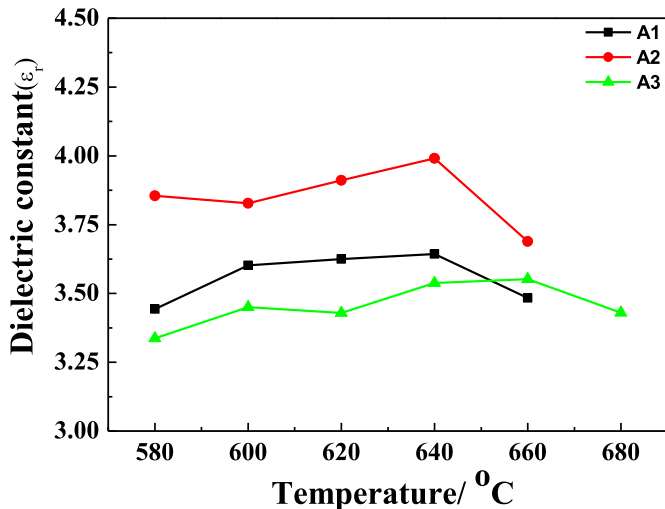


Fig. 4. Dielectric constants of CZBLglass/ Al_2O_3 composites as a function of firing temperatures.

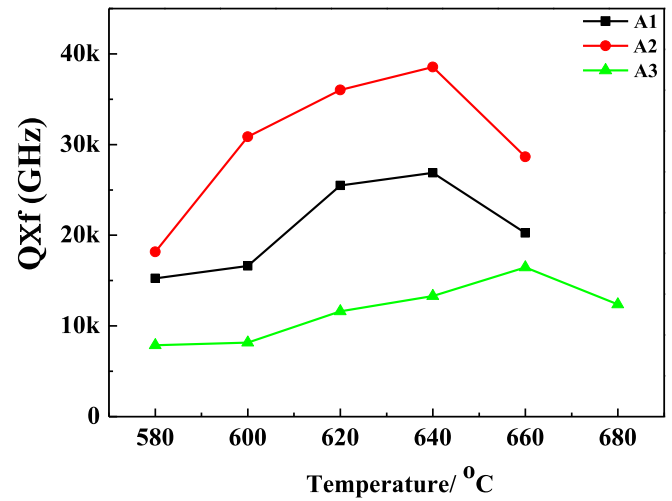


Fig. 5. The $Q \times f$ values of A1, A2 and A3 sintered at different temperatures.

increasing and reaches the maximum value and then decreases. At low sintering temperature, the samples have lower ϵ_r due to the more pores. It is reasonable for the composite with high Al_2O_3 ceramic filler to have a lower ϵ_r attributing to poor densification and amounts of pores. In a word, the permittivity of the composite lies on not only firing temperature but also phase composition.

The $Q \times f$ values of CZBL glass/ Al_2O_3 composites sintered at different temperatures are exhibited in Fig. 5. As for all samples, with the increase of sintering temperature, the $Q \times f$ values firstly increase and then decrease, and the sample A2 sintered at 640 °C has the maximum $Q \times f$ value of 38557 GHz. This result is well consistent with that of the bulk density seen in Fig. 2. With the sintering temperature increasing, the grain growth and the pore decrease have advantage to reduce the dielectric losses. And high content of Al_2O_3 ceramic filler will result in the decrease of $Q \times f$ value because of low densification.

Fig. 6 shows the τ_f values of CZBL glass/ Al_2O_3 composites at different temperatures. The τ_f values of all the composite samples change from -5.2 ppm/°C to 0.25 ppm/°C, and a near-zero τ_f value is obtained for the sample sintered at 640 °C. With the increase of Al_2O_3 content in the composites, the τ_f value of the samples slightly shifts to negative value due to the introduction of Al_2O_3 with large negative τ_f value (~ 60 ppm/°C). It is observed that the τ_f value is increased with the increment of sintering temperature, which may be due to the increase of $\text{Cu}_2\text{Al}_6\text{B}_4\text{O}_{17}$, $\text{Li}_2\text{CuB}_4\text{O}_8$ and CuB_2O_4 phases with low negative τ_f value.

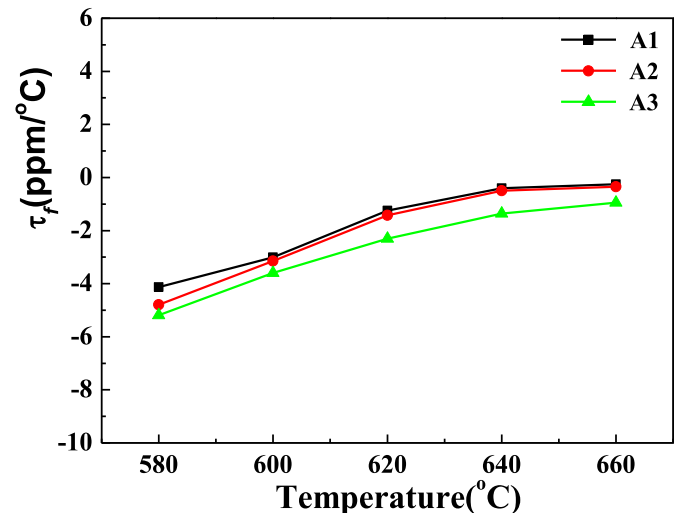


Fig. 6. The τ_f of A1, A2 and A3 sintered at different temperatures.

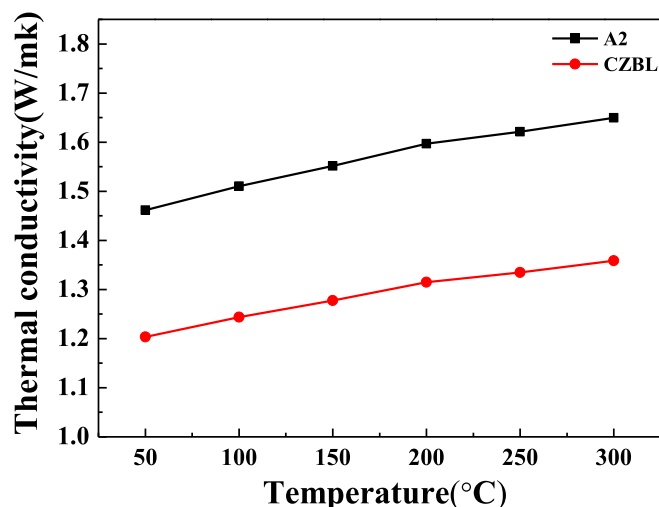


Fig. 7. Thermal conductivity values of the CZBL glass and A2 sintered at 640 °C as a function of testing temperature.

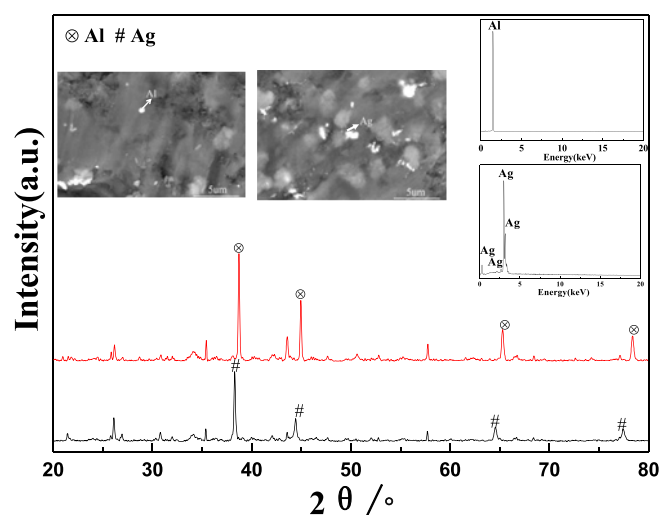


Fig. 8. XRD patterns, SEM images of the as-fired surface and EDS analysis result of CZBL/ Al_2O_3 composites co-fired with 20 wt% Ag and 20 wt% Al powders at 640 °C for 1 h, respectively.

Fig. 7 exhibits the thermal conductivity values of the CZBL glass and the sintered composite at different testing temperatures. It is observed that the thermal conductivity of these two materials increases linearly with the temperature increasing. The increase in thermal conductivity may be attributed to phonon collisions increased. As we know, the thermal conductivity of solids can be considered as the propagation of non-resonant elastic waves through the continuous medium, i.e., the interaction between the thermal quantum of phonons. The thermal conductivity mainly depends upon the average free path of the phonon. The greater the average free path of phonons, the higher the thermal conductivity. As for glass materials with a completely amorphous structure, its average free path of the phonon is limited to the order of magnitude of the atomic spacing because of irregular network structure, which is significantly smaller than that of crystals. So, the glass material has low thermal conductivity compared with crystals. Since Al_2O_3 has high thermal conductivity of 29.3 W(mK)^{-1} [28], according to composite material rule, the composite has a larger thermal conductivity than that of the CZBL glass.

To determine whether the composite is chemically compatible with Ag and Al electrodes, The CZBL glass/ Al_2O_3 composites were co-fired with 20 wt% Ag and 20 wt% Al at 640 °C for 1 h, respectively. The XRD

and SEM images of the co-fired specimens are exhibited in Fig. 8. From SEM and EDS results, a clear interface can be observed, suggesting that there is hardly any reaction between the electrodes and composite. The XRD patterns shown in Fig. 8 also confirm that there is no new phase emerging, indicating that the composite can be co-fired with the electrodes at ultra-low sintering temperature.

4. Conclusions

In this work, CZBL/ Al_2O_3 composites for LTCC applications were produced by solid-state reaction method, and the sintering, microstructure, physical properties were discussed. Several crystalline phases of $\text{Cu}_2\text{Al}_6\text{B}_4\text{O}_{17}$, $\text{Li}_2\text{CuB}_4\text{O}_8$ and CuB_2O_4 are formed during sintering process. The sample containing 10 wt% Al_2O_3 sintered at 640 °C displays an ultra-low ϵ_r of 3.79, a $Q \times f$ value of 38557 GHz and a near-zero resonance frequency temperature coefficient. Furthermore, the as-prepared composites can meet the requirements of good chemical compatibility with Ag and Al electrodes. Hence, it indicates that the composite is a promising material for ULTC technology, especially in the high frequency field.

Acknowledgments

This work was supported by the Natural Science Foundation of Guangxi Province, China (Grant no. 2018GXNSFBA281001).

Appendix A. Supplementary data

Supplementary data to this article can be found online at <https://doi.org/10.1016/j.ceramint.2019.08.166>.

References

- [1] F.L. Wang, W.J. Zhang, X.Y. Chen, Synthesis and characterization of low CTE value $\text{La}_2\text{O}_3\text{-B}_2\text{O}_3\text{-CaO-P}_2\text{O}_5$ glass/cordierite composites for LTCC application, *Ceram. Int.* 45 (2019) 7203–7209.
- [2] D.H. Jiang, J.J. Chen, B.B. Lu, J. Xi, G.H. Chen, Preparation, crystallization kinetics and microwave dielectric properties of $\text{CaO-ZnO-B}_2\text{O}_3\text{-P}_2\text{O}_5\text{-TiO}_2$ glass-ceramics, *Ceram. Int.* 45 (2019) 8233–8237.
- [3] F.L. Wang, X.Y. Chen, W.J. Zhang, H.J. Mao, Synthesis and characterization of borosilicate glass/ β -spodumene/ Al_2O_3 composites with low CTE value for LTCC applications, *J. Mater. Sci. Mater. Electron.* 29 (2018) 9038–9044.
- [4] C.W. Wu, J.H. Jean, Crystallization kinetics and dielectric properties of a low-fire $\text{CaO-Al}_2\text{O}_3\text{-SiO}_2$ glass + alumina system, *J. Am. Ceram. Soc.* (2016) 1–8.
- [5] R.R. Tummala, Ceramic and glass-ceramic packaging in the 1990s, *J. Am. Ceram. Soc.* 74 (1991) 895–908.
- [6] M.T. Sebastian, H. Jantunen, Low loss dielectric materials for LTCC applications: a review, *Int. Mater. Rev.* 53 (2008) 57–90.
- [7] D.H. Jiang, J.J. Chen, B.B. Lu, A new glass-ceramic with low permittivity for LTCC application, *J. Mater. Sci. Mater. Electron.* 29 (2018) 18426–18431.
- [8] H.T. Yu, L. He, M.S. Zeng, J.S. Liu, E.Z. Li, X.H. Zhou, S.R. Zhang, Low temperature sintering of $\text{Zn}_{1.8}\text{SiO}_{3.8}$ dielectric ceramics containing 3ZnO-2B₂O₃ glass, *Mater. Lett.* 179 (2016) 150–153.
- [9] X.F. Luo, L.C. Ren, Y.S. Xia, Y.K. Hua, W.Y. Gong, M.C. Cai, H.Q. Zhou, Microstructure, sinterability and properties of $\text{CaO-B}_2\text{O}_3\text{-SiO}_2$ glass/ Al_2O_3 composites for LTCC application, *Ceram. Int.* 43 (2017) 6791–6795.
- [10] M.S. Ma, Z.Q. Fu, Z.F. Liu, Fabrication and microwave dielectric properties of $\text{CuO-B}_2\text{O}_3\text{-Li}_2\text{O}$ glass-ceramic with ultra-low sintering temperature, *Ceram. Int.* 43 (2017) S292–S295.
- [11] A. Bittner, A. Ababneh, H. Seidel, U. Schmid, Influence of the crystal orientation on the electrical properties of AlN thin films on LTCC substrates, *Appl. Surf. Sci.* 257 (2010) 1088–1091.
- [12] Y. Kobayashi, Low-temperature fabrication of anorthite ceramics, *J. Am. Ceram. Soc.* 77 (1994) 833–834.
- [13] S. Arcaro, F.R. Cesconeto, F. Raupp-Pereira, Synthesis and characterization of LZS/ $\alpha\text{-Al}_2\text{O}_3$ glass-ceramic composites for applications in the LTCC technology, *Ceram. Int.* 40 (2014) 5269–5274.
- [14] H.T. Yu, J.S. Liu, W.L. Zhang, Ultra-low sintering temperature ceramics for LTCC applications: a review, *J. Mater. Sci. Mater. Electron.* 26 (2015) 9414–9423.
- [15] Z.J. Qing, The effects of B_2O_3 on the microstructure and properties of lithium aluminosilicate glass-ceramics for LTCC applications, *Mater. Lett.* 212 (2018) 126–129.
- [16] X.F. Luo, L.C. Ren, Y.K. Hua, Y.S. Xia, M. Xin, C. Zhang, H.Q. Zhou, Fabrication and performance of dielectric tape based on $\text{CaO-B}_2\text{O}_3\text{-SiO}_2$ glass/ Al_2O_3 for LTCC applications, *Ceram. Int.* 44 (2018) 6354–6361.

- [17] M. Okamoto, H. Kodama, K. Shinozaki, Effect of alkali metal oxide addition on the sinterability of $\text{MgO-B}_2\text{O}_3\text{-Al}_2\text{O}_3$ glass- Al_2O_3 filler composites, *J. Am. Ceram. Soc.* 91 (2008) 1110–1114.
- [18] N. McN. Alford, S.J. Penn, Sintered alumina with low dielectric loss, *J. Appl. Phys.* 80 (1996) 5895–5898.
- [19] S.J. Perm, N.M. Alford, A. Templeton, Effect of porosity and grain size on the microwave dielectric properties of sintered alumina, *J. Am. Ceram. Soc.* 80 (1997) 1885–1888.
- [20] H.T. Yu, J.S. Liu, W.L. Zhang, S.R. Zhang, Ultra-low sintering temperature ceramics for LTCC applications: a review, *J. Mater. Sci. Mater. Electron.* 26 (2015) 9414–9423.
- [21] H.T. Yu, K. Ju, K.M. Wang, A novel glass-ceramic with ultra-low sintering temperature for LTCC application, *J. Am. Ceram. Soc.* 97 (2014) 704–707.
- [22] S. Fujino, C. Hwang, K. Morinaga, Density, surface tension, and viscosity of $\text{PbO-B}_2\text{O}_3\text{-SiO}_2$ glass melts, *J. Am. Ceram. Soc.* 87 (2004) 10–16.
- [23] M.S. Ma, Z.Q. Fu, Z.F. Liu, Fabrication and microwave dielectric properties of $\text{CuO-B}_2\text{O}_3\text{-Li}_2\text{O}$ glass ceramic with ultra-low sintering temperature, *Ceram. Int.* 43 (2017) S292–S295.
- [24] X.Y. Chen, F.L. Wang, W.J. Zhang, Low temperature sintering and dielectric properties of $\text{La}_2\text{O}_3\text{-B}_2\text{O}_3\text{-Al}_2\text{O}_3$ glass-ceramic/ Al_2O_3 composites for LTCC applications, *J. Mater. Sci. Mater. Electron.* 30 (2019) 3098–3106.
- [25] J. Xi, B.B. Lu, J.J. Chen, G.H. Chen, F. Shang, J.W. Xu, C.R. Zhou, C.L. Yuan, Ultralow sintering temperature and permittivity with excellent thermal stability in novel borate glass-ceramics, *J. Non-Cryst. Solids* 521 (2019) 119527.
- [26] P.A. Plachinda, E.L. Belokonevab, Synthesis and crystal structure of commensurate polymorph of $\text{Ln}_4\text{AlCu}_2\text{B}_9\text{O}_{23}$ ($\text{Ln} = \text{Lu}, \text{Ho}$) and refinement of $\text{Cu}_2\text{Al}_6\text{B}_4\text{O}_{17}$, *Z. Anorg. Allg. Chem.* 634 (2008) 1965–1970.
- [27] C.C. Zhu, X.Y. Nai, D.H. Zhu, F.Q. Guo, Y.X. Zhang, W. Li, Growth process of $\text{Cu}_2\text{Al}_6\text{B}_4\text{O}_{17}$ whiskers, *J. Solid State Chem.* 197 (2013) 1–6.
- [28] R. Berman, The thermal conductivities of some dielectric solids at low temperatures (experimental), *Proc. R. Soc. Lond. A.* 208 (1951) 90–108.